

LIFE CYCLE ASSESSMENT OF FRP SEISMIC RETROFITTING

Sarah V. Russell-Smith and Michael D. Lepech

Department of Civil Engineering and Environmental Engineering, Stanford University, California, USA

ABSTRACT

The seismic retrofitting of transportation infrastructure to ensure public safety and network connectivity following a large magnitude earthquake is a multi-year and multi-billion dollar investment for infrastructure owners and managers worldwide. In California alone, seismic retrofitting of vulnerable bridges will cost Caltrans over US\$8 billion when complete. While many researchers and managers have looked at minimizing the economic costs of retrofitting applications, both initial and life cycle, of various retrofitting choices, differences in sustainability among these choices has yet to be quantified and weighed. In this research, the annualized sustainability impacts of a number of retrofitting strategies are explored using infrastructure fragility curves. Findings show a number of environmental impacts resulting from each retrofitting strategy, enabling infrastructure managers to consider more than just economic costs when designing and constructing seismic retrofit applications.

Keywords: sustainability, FRP, retrofitting, fragility, seismic, infrastructure

1 INTRODUCTION

As noted by numerous researchers, a number of relatively recent destructive earthquakes (i.e. 1989 Loma Prieta, 1994 Northridge, 1995 Hanshin-Awaji) have inflicted serious damage on our transportation networks [1,2,3]. The majority of serious damage has occurred on bridge structures, identifying them as the most vulnerable components of our transportation systems [4]. Damage to bridge structures, which often serve as singular points of crossing in an otherwise highly connected transportation network, can result in significant long-term disruptions in general mobility (both personal and freight) along with acute interruptions in emergency response and recovery.

In response to this high vulnerability, many state departments of transportation in the US, and ministries of transportation internationally, have engaged in extensive bridge retrofitting programs to enhance the reliability, safety, and robustness of transportation networks. As an example following the 1989 Loma Prieta earthquake, a total of 1,039 state-owned bridges within California were identified as "in need of being retrofitted to meet seismic safety standards" [5]. Following Northridge in 1994 an additional 1,155 were added to this group. In total, the State of California has identified approximately 2,200 bridges that are in need of seismic retrofitting at a cost of over US\$8.4 billion.

1.1 Approaches to Seismic Retrofitting

A number of techniques are being used to seismically harden the extensive transportation system. Within California, the seismic retrofitting of bridge structures primarily consists of strengthening the support columns of existing structures by encasing particularly critical columns with a steel casing or, in some instances, an advanced fiber composite casing. In addition to this commonly prescribed column "jacketing" procedure, a number of other retrofitting techniques are also carried out separate from or in addition to column work. In some cases, bridge footing sizes are increased and bolstered by placing additional pilings underground or by using steel tie-down rods to better anchor the footings to pilings or supporting soil. In some projects, bridge abutments are made larger and the existing structural restraint units are strengthened. This may be necessary to account for increasing stiffness and loads passed into the abutments due to encasement of columns.

Apart from column and associated abutment strengthening, many retrofits also involve "hinge seat extensions" which enlarges the size of the hinges that connect sections of bridge decks and prevents them from separating during severe ground movement [5]. Regardless of the type of retrofit implemented, the actual design of retrofits cannot be generalized, but rather is unique among sites and based on the maximum credible earthquake (MCE) expected at that location. In sum, the exact retrofitting solution

depends on many factors, including proximity to the nearest known active fault, the type of geology and other soil conditions present at the site, and the seismic resistance of the original structural design along with any design changes that have taken place throughout service life.

As mentioned previously, within California the seismic retrofitting of bridge structures consists largely of column jacketing. Earlier concrete column designs have been demonstrated to lack the flexural strength, flexural ductility, and shear strength necessary to resist extreme seismic loads [2]. Seible et al [6] attributed these deficiencies to a number of mechanisms including: (a) inadequacy of transverse reinforcement leading to brittle shear failure, (b) poor confinement in flexural plastic hinge regions, and (c) poor detailing in lap splices at the lower ends of columns. A number of column jacketing approaches have been successfully applied including steel jacketing, wire prestressing, and composite material jacketing. To date, steel jacketing has been the most widely adopted bridge retrofit technique [2].

1.2 Steel Jacketing of Concrete Columns

Steel jacketing of columns is comprised of a two-step application process. Initially a tube of steel is placed around the column (circular columns are commonly fitted) by fitting two half shells of steel plate that is rolled to a radius only slightly larger than the existing column. These two half shells are then field-welded together along the vertical seam to produce a continuous tube around the column. The second step of this process is grouting of the annular gap between column and jacket with mortar or a pure cement compound. This grouting serves to partially bond the jacket to the existing column and function as effective passive confinement. As noted by Kim and Shinozuka [2], it is important that the steel jacket is cut to provide a space of about 50mm between the jacket and any supporting members framing into the retrofitted column. This avoids the possibility of the jacket acting as compression reinforcement through bearing of the supporting members at large drift angles. A typical seismic retrofitting detail for a reinforced concrete column using a steel jacket is shown in Figure 1.

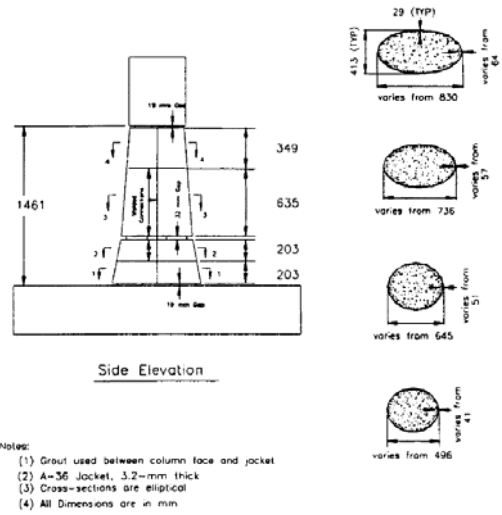


Figure 1: Example seismic retrofitting detail for a reinforced concrete column using a steel jacket [7]

1.3 FRP Jacketing of Concrete Columns

Composite material jackets or fiber reinforced polymer (FRP) jackets can be commonly applied by two methods, either as wet lay-up or as a prefabricated system [6]. The wet lay-up process can entail the use of dry sheets or woven fabrics of fiber reinforcement (i.e. glass, carbon) being impregnated with polymer resin on site, the application of pre-impregnated sheets or fabrics with or without additional resin, or the impregnation of dry tows (untwisted bundles of continuous fibers) with resin during the winding process. Prefabricated systems are similar to steel jackets in that they are comprised of split shells that are fitted and joined around columns [6]. The wet lay-up process can be carried out manually through hand application of fiber sheets or automatically through machine wrapping of individual fiber tows around the circumference of the column. Unstressed or prestressed applications also exist for both wet lay-up and prefabricated techniques. The automated FRP wrapping of a reinforced concrete bridge pier column is shown in Figure 2. A typical seismic retrofitting detail for a reinforced concrete column using an FRP jacket is shown in Figure 3.



Figure 2: Automated FRP wrapping of a reinforced concrete bridge column (courtesy of Xxsys Technologies)

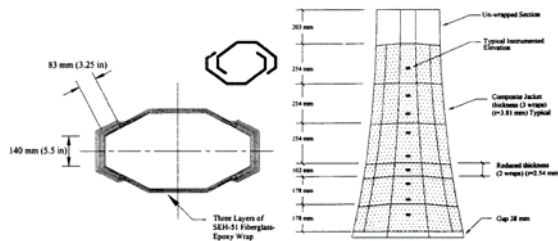


Figure 3: Example seismic retrofitting detail for a reinforced concrete column using a FRP jacket [7]

1.4 Effectiveness of Column Retrofitting

A significant number of studies, both by departments and ministries of transportation and by academic researchers, have compared the effects of using steel and FRP jacketing to strengthen structures prior to a major seismic event (pre-event strengthening) and to repair damaged bridge columns following a major event (post-event repair). In the case of steel jacketing for concrete columns, Chai et al [8], Prestley et al [9], and Ghojarah et al [10] found that the use of steel jackets can significantly improve the flexural capacity of retrofitted columns and connections. Similar results have been found for FRP-wrapped columns [6,11,12]. Bakis et al [13] noted that epoxy-bonding of FRP materials with fiber reinforcement parallel to the principle tensile stresses can effectively improve shear strength. Additionally, FRP wrapping of circular columns effectively curtails the lateral expansion of concrete shortly after the unconfined strength has been reached [13].

While these individual examples of the success of steel and FRP jacketing are compelling, Youm et al [14] carried out a series of directly comparative experimental tests to determine the effectiveness of

both steel jacketing and FRP wrapping of reinforced concrete columns at improving shear strength, flexural ductility, and seismic performance of repaired columns (post-event repair).

Within that study, Youm et al constructed a series of nine RC column specimens with three different transverse reinforcement ratios. All columns were designed in accordance with the American Association of State and Highway Transportation Officials (AASHTO) Standard Specification for Highway Bridges. Circular columns were 300mm in diameter and 2200mm in height, with 1.26% longitudinal reinforcement ratio, 17.9 MPa concrete, and transverse reinforcement ratios between 0.6% and 2.1%.

Figures 4, 5, and 6 from Youm et al show the cyclic loading loops for the damage-free column (initial damage loading), the steel jacketed repaired column, and the FRP jacketed repaired column, respectively. As seen, while the steel jacket repair shows better energy dissipation capacity than the FRP jacket repair, both significantly increase the strength and ductility of damaged columns.

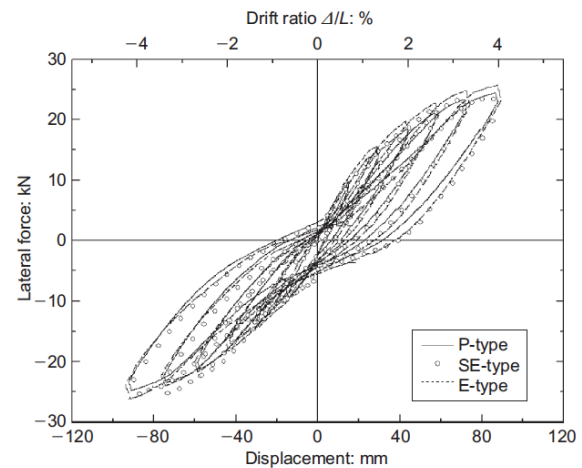


Figure 4: Cyclic loading loops of undamaged reinforced concrete columns [14]

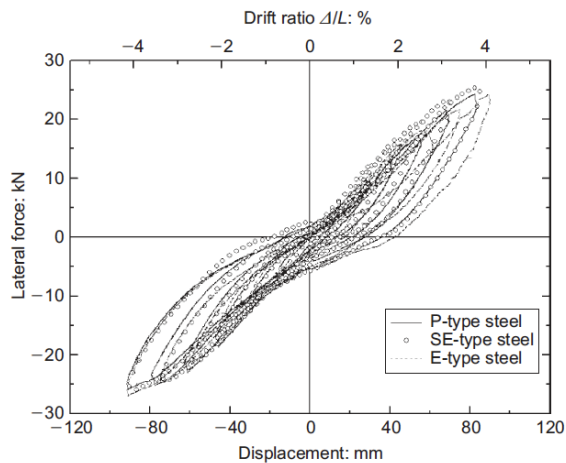


Figure 5: Cyclic loading loops of repaired reinforced concrete columns with steel jacketing [14]

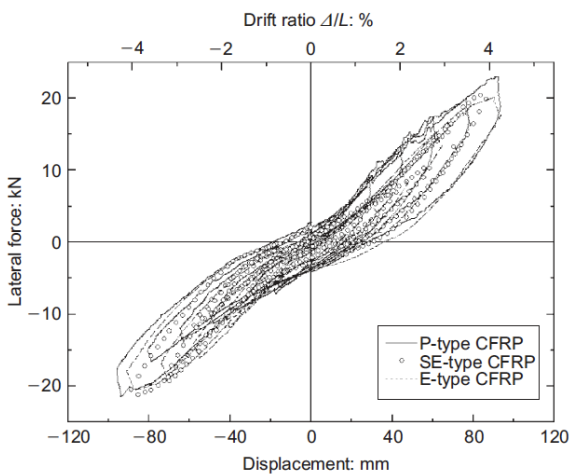


Figure 6: Cyclic loading loops of repaired reinforced concrete columns with FRP jacketing [14]

From these studies, we find that steel and FRP jacketing of columns can both lead to effective improvement of shear strength, flexural strength, flexural ductility, and concrete confinement in bridge column applications. As mentioned previously, to date most jacketing retrofits have been completed using steel jackets due to matters of initial cost, construction ease, and wider familiarity with steel construction materials and methods.

2 LIFE CYCLE ASSESSMENT OF RETROFIT TECHNIQUES

Life cycle assessment (LCA) is an analytical framework for measuring environmental and social impacts of a product system or technology by evaluating the inputs and outputs of a product or process throughout its life cycle, including raw material acquisition, production, use, final disposal or recycling, and transportation needed between

these phases [14]. A generalized framework of process-based life cycle assessment that captures measurement of all inputs and outputs of a system is shown in Figure 7.

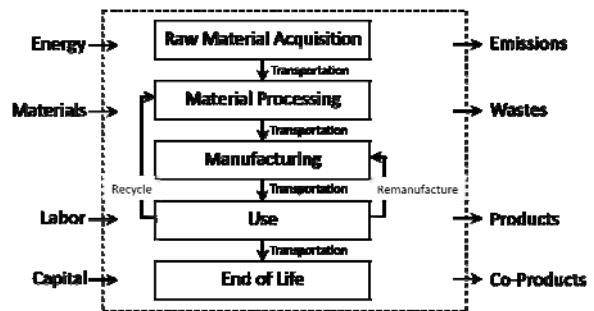


Figure 7: Generalized framework for life cycle assessment (LCA) of systems

Apart from life cycle assessment, life cycle cost assessment (LCCA) is a technique for total cost accounting and a complementary methodology to life cycle assessment. LCCA uses life cycle principles to augment conventional cost analyses by estimating not just initial costs, but also use and disposal costs. In this study, the economic life cycle costs of various seismic retrofitting alternatives will not be discussed in great detail. Such analysis has been carried out by Kappos and Dimitrakopoulos [16] for pre-event strengthening of buildings. Within this preliminary work, life cycle assessment indicators will concentrate primarily on environmental damage and resource intensity indicators.

2.1 Life Cycle Inventory of Retrofit Techniques

The foundation of all life cycle assessments are the life cycle inventories that comprise the total inputs (energy, materials, labor, capital) and outputs (emissions, wastes, products, co-products) associated with every component piece and process that makes up the entire system from raw material acquisition to end-of-life. Within this work, three retrofitting alternatives are compared. These are steel jacketing, FRP jacketing using epoxy resin, and FRP jacketing using unsaturated polyester resin. Prior to starting the overall assessment and undertaking a comparison of all three systems, a life cycle inventory (LCI) for unsaturated polyester resin manufactured in the US was needed.

(2.1.1) Life Cycle Inventory of Unsaturated Polyester Resin (UPR), Epoxy, and Steel Materials

A cradle-to-gate LCI analysis of unsaturated polyester resin (UPR) was carried out. The use and end of life phase of UPR are not quantified in the LCI. Since such a life cycle inventory does not currently exist, the goal of this LCI is to generate an LCI of UPR based on U.S data and compare the environmental burden of UPR with epoxy resin to

quantify the relative sustainability of each on an equal mass basis for use in the larger assessment of seismic retrofitting. In the case of UPR, data is based on that of a large U.S. based producer and is representative of UPR production in the U.S. in general. In the case of missing or proprietary information, certain assumptions are made; these assumptions introduce a certain degree of uncertainty to the UPR LCI results.

There have been several approaches to LCIA that have been discussed critically including Hofstetter [16], Bare and Gloria [17], ISO 14040 [14], and most recently the European Commission's International Reference Life Cycle Data System (ILCD) Handbook: Specific guidance document for generic or average Life Cycle Inventory (LCI) data sets [18]. In this LCI, we used the approach described by the ILCD Handbook. The approach taken is an iterative approach in which the goal is defined, the scope specified to match the goal, the process of the system modeled roughly and then improved until accuracy, precision, and completeness correspond to the goal and scope which may also require some revision [18].

The data set compiled can be generic, representing the typical range of deviation, or average, representing actual average for process/product [18]; in this study a generic data set is compiled. Further, the data set must correspond to a specific time and geographic region; in this case, 2009 and the United States. For this approach, six primary aspects of inventory data quality are defined in accordance with ISO 14044: technological representativeness, geographical representativeness, time representativeness, completeness, precision/uncertainty, and methodological appropriateness/consistency [18].

The completed LCI contains disaggregate results, which are then used to determine the environmental impact of the process/product based on several impact categories. This can be done with either the mid-point (impact potential) or the end-point (damage) factors; in this analysis mid-point factors are used. Mid-point impact categories include global warming potential (GWP), primary energy (PE), acidification potential, eutrophication potential, human toxicity potential, ozone layer depletion potential, and photochemical smog formation potential.

For each category, the LCIA results are calculated by multiplying the amount of each relevant LCI flow by a characteristic weighting factor and then summing all the values [18]. GWP is calculated in terms of carbon dioxide (CO₂) equivalent on a mass basis for a given time period. For example, 1 kilogram (kg) of nitrous oxide has a GWP equivalent to 298 kg of CO₂ on a 100-year timescale; 1 kg of methane has a GWP equivalent to 25 kg of CO₂ on a 100-year timescale [19].

Characteristic weighting factors for the different impact categories can be found in the literature.

(2.1.2) Process Description

It is important to understand the general process of UPR production including material inputs, energy inputs, by-products, and production process. Production involves 6 stages and several chemical components with the main derivatives being maleic anhydride, propylene glycol, styrene, and isophthalic acid. During production the resin moves from chemical reactor to thinning tank, to storage tank, to blending tank, back to storage tank, until it is shipped for use. This is shown graphically in Figure 8.

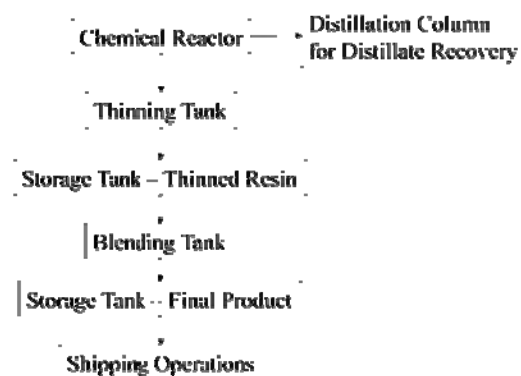


Figure 8: Schematic outline of the unsaturated polyester resin (UPR) production process

In the chemical reactor the anhydrides are combined with diols. The first step is the formation of the half-ester, which takes place rapidly. The second step is the formation of the full-ester which is both energy intensive and water intensive, with water constantly removed by distillation for the reaction to advance. The distillation process generates undesirable distillate byproducts composed of approximately 7% organics. The distillate byproducts are re-distilled to recover 3% organics in the form of glycols which are then recycled. The final distillate contains 4% organics and is burned in an incinerator. Energy is required to mix the chemical reactor, maintain reaction temperature of 200°C, and vaporize water to form full ester.

Resin then enters the thinning tank via gravity and mixes with styrene. The resin is cooled from 200°C to 80°C, the maximum temperature allowed to prevent side reactions. The styrene vapors are captured and sent to an incinerator. Energy is required to mix and cool the resin.

The resin then enters a storage tank where multiple batches can be held. Styrene vapors are continuously vented to the incinerator. The resin is then moved to the blending tank where it is combined with additives. The additives are used to achieve the desired properties and vary depending on the intended application of the resin. After

blending, the final product is held in storage tanks until shipped via tank truck or rail car.

End-use application of the product involves mixing the resin with a curing agent, pouring into a mold, waiting for resin to cure at room temperature (minutes), removing the mold, and then the resin is ready for use. Unsaturated polyester is a thermoset resin: it cannot be melted again once it is cured, but can be recycled into other applications.

(2.1.3) Process and Life Cycle Data

As stated in section 2.1.2, some assumptions were made in the generation of the UPR LCI. These assumptions as well as data sources and LCI process boundaries are included below.

The basis of all calculations was initially 1000 kg of unthinned resin and later a conversion factor was used, changing the basis to 1 kg of final product UPR resin. Energy requirements included differentiation between delivered energy and site energy as well as between heat (kJ) and electrical energy (kJe).

In order to calculate energy requirements of the UPR process it was assumed that the efficiency of the industrial natural gas burner is 78% of LHV based on data from plant flue gas with 10% excess air. Efficiencies of mixing motors were assumed to be similar to 3-phase induction motors operating at 1800 rpm.

- 1 HP at 100% load – 72%
- 20 HP at 50% load – 85%
- 15 HP at 50% load – 82%
- 10 HP at 50% load – 82%

The LCI template used for the chemical constituents of UPR including propylene glycol, maleic anhydride, isophthalic acid, styrene, as well as diesel for transport is based on the Association of Plastics Manufacturers Europe (APME) LCI template [20]. Catalysts for the chemical reactor and additives (in the blending tank) were not included as these materials represent less than 1% of the total material and negligible environmental impact. In general, any process/constituent that corresponded to less than 5% of the overall impact of UPR production and not an acute human or ecological health risk was considered outside the boundary of this study.

Styrene data came directly from APME [20]; propylene glycol data came from The Engineering Society for Advancing Mobility Land, Sea, Air and Space [21]; maleic anhydride data came from Domènech, Ayllón and Peral’s paper “How Green Is a Chemical Reaction? Application of LCA to Green Chemistry” [22]; rail and truck diesel transportation data came from Franklin and Assoc. Ltd [23]; natural gas data came from SimaPro life cycle assessment software [24]; and electricity emissions data came from Kim and Dale’s article “Life Cycle Inventory

of the United States Electricity System” [25]. Isophthalic acid LCA data was unavailable. The LCI for each constituent was completed using identical simplified APME templates so that all data groups could be summed for the total LCI of UPR.

The mid-point impact categories were then used to aggregate the results. As noted previously, the impact categories utilized are primary energy consumption (denoted PE measured in MJ) and global warming potential (denoted GWP measured in kg CO₂-eq). The characteristic weighting factors for calculating GWP came from the Intergovernmental Panel on Climate Change (IPCC) Fourth Assessment Report [19]. The GWP and PE impacts of UPR were compared to that of epoxy resin on a mass basis. The epoxy resin data came from SimaPro life cycle assessment software [24]. The resulting analysis and conclusions are shown below based on the sustainability metrics of PE consumption and GWP.

(2.1.4) LCI Results

Selected LCI results for UPR obtained from this primary LCI construction are shown in Table 1. The primary energy and global warming potential intensities determined for UPR are juxtaposed with the PE and GWP data from SimaPro for epoxy resin and glass fiber, common constituents of fiber reinforced polymers (FRP), along with rolled plate steel and cement mortar (both used in steel jacketing for reinforced concrete columns).

Table 1: LCI results per kg of UPR, epoxy resin, glass fiber, rolled steel plate, and cement mortar in terms of primary energy and global warming potential impact categories

	GWP (kg CO ₂ e)	PE (MJ)
UPR	2.82	62.1
Epoxy resin	1.11	236
Glass fiber	0.508	8.67
Rolled Steel plate	0.998	20.5
Cement mortar	0.13	0.85

(2.1.5) Life Cycle Inventory of UPR, Epoxy, and Steel Retrofit Systems

Using the basic life cycle inventories for the unsaturated polyester resin FRP, epoxy-based resin FRP, and steel materials, life cycle inventories of the in-place impacts of these retrofit strategies can be computed. To do this, three different retrofit designs were produced to provide approximately equivalent behavior in the structural system. The thickness of the steel jacket was determined using the stress-strain relationships of confined reinforced concrete detailed by Mander et al [27] and shown as

Equation 1.

$$t_j = \frac{0.18(\varepsilon_{cc} - 0.004)Df'_{cc}}{f_{yj}\varepsilon_{sm}} \quad (1)$$

where, t_j is the jacket thickness, ε_{cc} is the ultimate compressive strain, D is the column diameter, f'_{cc} is the compressive strength of the confined concrete, f_{yj} is the yield strength of the jacket, and ε_{sm} is the jacket strain at ultimate stress.

A similar equation proposed by Seible et al [6] was used to compute the FRP jacket thicknesses and is shown as Equation 2.

$$t_j = \frac{0.1(\varepsilon_{cc} - 0.004)Df'_{cc}}{f_{CFS}\varepsilon_{fr}} \quad (2)$$

where, t_j is the jacket thickness, ε_{cc} is the ultimate compressive strain, D is the column diameter, f'_{cc} is the compressive strength of the confined concrete, f_{CFS} is the tensile strength of the FRP in the hoop direction, and ε_{fr} is the ultimate strain of the FRP.

For the design and evaluation of seismic retrofitting techniques, a specific example bridge is adopted from Kim et al [2] for the design of steel jacketed and FRP wrapped column retrofits. The structural layout and details are shown in Figure 9.

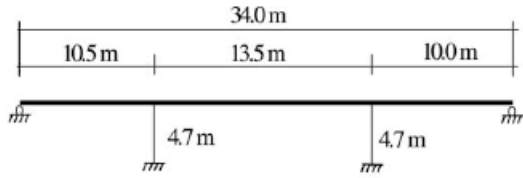


Figure 9: Elevation of the example bridge [2]

As noted by Kim et al, this bridge has an overall length of 34.0 meters, make up of 3 spans. The superstructure is made up of a longitudinally reinforced concrete deck 10 meters wide and supported by two pairs of columns and an abutment at each end. Each column support has three circular columns with a diameter of 800 millimeters. Additional details on the structural makeup of this sample bridge can be found in Kim et al [2].

Following Shinozuka et al [3] and Yuom et al [14], the AASHTO recommended design target of 34.3 MPa confined concrete compressive strength and a confining stress of 3.0 MPa were selected to compute the retrofitting design requirements. A column diameter of 800mm from the bridge in Figure 9 was used. Based on Equations 1 and 2, a steel jacket thickness of 2.0 millimeters, epoxy FRP jacket thickness of 0.33 millimeters, and a UPR epoxy jacket thickness of 0.45 millimeters (800g/m² fiber content) were required. The steel jacket is

bonded to the column with a 25mm thick layer of cement mortar surrounding the column. The FRP retrofit systems are bonded directly to the column face. The total global warming potential and primary energy impacts per column for retrofitting the bridge are given in Table 2.

Table 2: LCI results per column retrofitting of UPR-based column wrapping, epoxy-based column wrapping, and steel column jacketing in terms of primary energy (PE) and global warming potential (GWP) impact categories

	GWP (kg CO ₂ e)	PE (MJ)
UPR-based Wrapping	15.9	339
Epoxy-based Wrapping	5.67	694
Steel Jacketing	277	4400

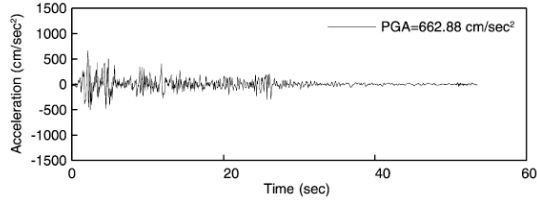
3 SUSTAINABILITY INDICATOR ESTIMATION BASED ON INFRASTRUCTURE FRAGILITY CURVES

With the LCI and system design complete, the quantification of sustainability indicators for seismic retrofitting begins with a probabilistic analysis of the seismic risk hazard, followed by a quantification of the structural vulnerability among the three retrofits, and finally an integration of risk, vulnerability, and environmental “cost” in terms of sustainability indicators to compare overall sustainability of comparable retrofit techniques. The assessment of seismic risk for distributed transportation networks has been investigated previously by Kiremidjian et al [28], Shinozuka et al [29], Werner et al [30], and others. While these studies have effectively explored the quantification and mitigation of seismic risk to distributed large-scale transportation networks, they have failed to incorporate the sustainability impacts of implementing seismic retrofitting and mitigation schemes. This research integrates the fundamental risk assessment and mitigation of seismic risk with efficient design and planning to achieve a specified level of safety with lower sustainability impacts throughout the retrofit service life.

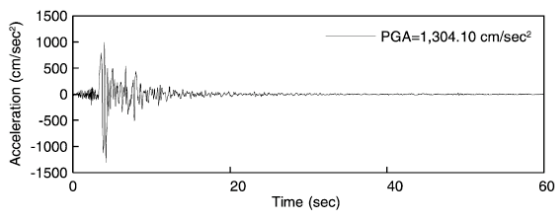
3.1 Seismic Risk

This analysis adopts the seismic risk profile used by Kim et al [2] for a specific bridge structure (Figure 9) located in Los Angeles County. In this case, 60 ground accelerations were taken for the Los Angeles area developed by the US Federal Emergency Management Agency SAC project. As noted by Kim et al, these acceleration time histories were derived from historical records of the Los Angeles

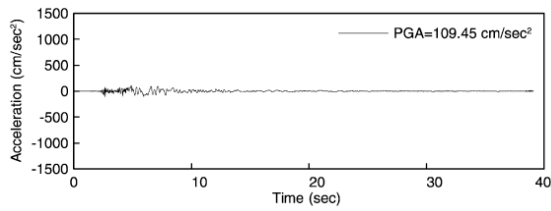
are with some linear adjustments and are made up of three groups of events having probabilities of exceedance of 10% in 50 years, 2% in 50 years, and 50% in 50 years. A typical acceleration time history is shown for each of these groups in Figure 10.



(a) 10% probability of exceedance in 50 years



(b) 2% probability of exceedance in 50 years



(c) 50% probability of exceedance in 50 years

Figure 10.: Typical ground acceleration time histories for Los Angeles [2]

In this analysis, these three events will be classified as (a) moderate, (b) strong, and (c) weak ground motions or events.

3.2 Structural Vulnerability

Along with seismic hazard, the quantification of structural vulnerability is essential to determining the impact of structural retrofitting in preventing damage or collapse from a given seismic event. Currently, many researchers are expressing this structural risk in the form of fragility curves based on analytic or statistical data [31]. Fragility curves are expressions of cumulative log-normal probability functions that correlate an intensity factor such as peak ground acceleration (PGA) to the probability that a building or structure will exceed a particular damage state.

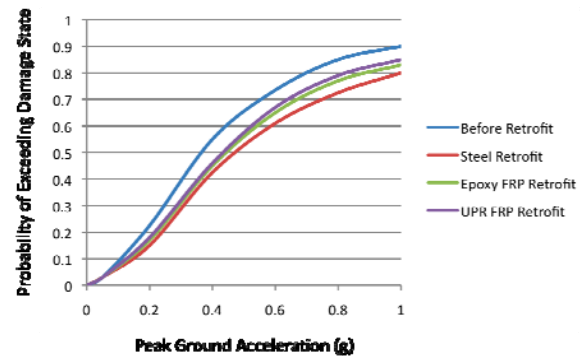
Following Shinozuka and Feng [32], a family of fragility curves were constructed for five given events

(E_1, E_2, E_3, E_4, E_5) indicative of no damage, slight damage, moderate damage, extensive damage, and complete collapse damage states. The probability $P_{ik} = P(a_i, E_k)$ indicates the probability that a bridge will be in damage state E_k when subjected a ground motion expressed by $PGA = a_i$. From this, Shinozuka and Feng have represented fragility curves as

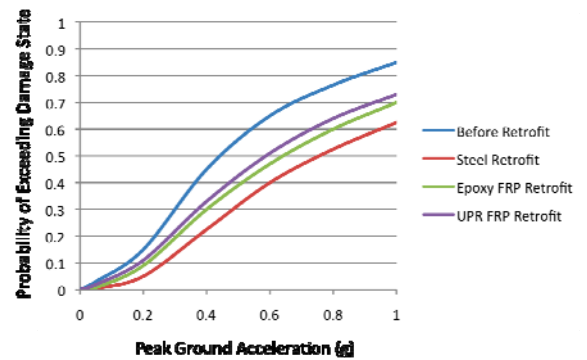
$$F_j(a_i; c_j, \zeta_j) = \Phi \left[\frac{\ln(a_i / c_j)}{\zeta_j} \right] \quad (3)$$

where Φ is the standard-normal distribution function, c_j is the median of the fragility curve for the damage state $j = 1, 2, 3, 4$ and ζ_j is the log-standard deviation of the fragility curve.

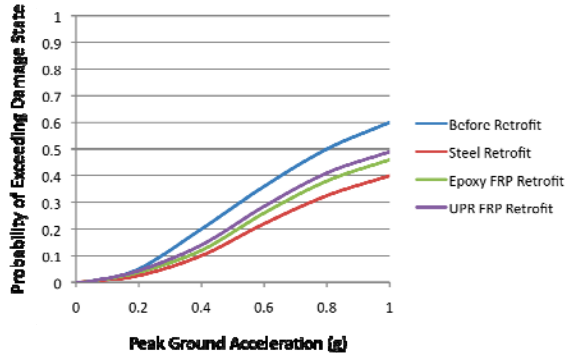
For the five damage states outlined previously, the fragility curves for the bridge structure before retrofit, after steel jacketing, and after wrapping with either epoxy-based FRP or UPR-based FRP are shown in Figure 11.



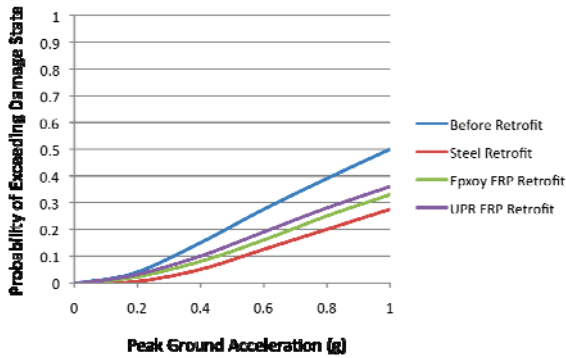
(a) No damage



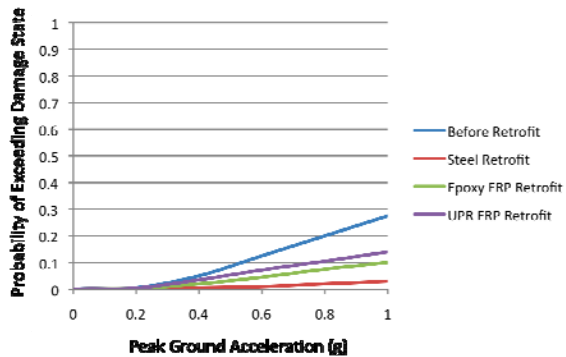
(b) Slight damage



(c) Moderate damage



(d) Extensive damage



(e) Complete collapse

Figure 11: Fragility curves of an example bridge (Figure 9) before retrofitting and after three different retrofits for a range of damage states from (a) no damage through (e) complete collapse

Similar to that done by Kim et al [2], the definitions of the damage states were drawn from Dutta and Mander [33]. From these damage state predictions, peak ductility demands for each damage state were calculated for each retrofit scenario. As seen, due to the lower modeled stiffness of the FRP materials compared to steel jacketing and the adoption of a displacement limit state (drift ratio), the fragility curves for the fiber reinforced polymer

systems lie above the steel retrofit curves in all circumstances. The curves for pre-retrofitted and steel retrofitted structures closely follow those by Kim et al [2].

3.3 Evaluation Using Life Cycle Analysis

As outlined in Kappos and Dimitrakopoulos [16] life cycle cost analysis has been used previously to determine the lowest economic cost of seismic retrofitting schemes. The procedure for this evaluation approach is provided in detail by Wen and Kang [34], Frangopol et al [35], and Liu et al [36]. As expressed by Ken and Wang, the expression for total life cycle expected cost over a time horizon, t , for a single hazard with respect to design variable, X , can be calculated as

$$E[C(t, X)] = C_0 + (C_1 P_1 + C_2 P_2 + \dots C_k P_k) \frac{N}{\lambda} \times (1 - e^{-\lambda t}) + \frac{C_m}{\lambda} (1 - e^{-\lambda t}) \quad (4)$$

where $E[]$ is the expected life cycle cost, $C()$ is the cost of a retrofit strategy, X , over a specified length of time, C_0 is the initial cost, C_k is the k^{th} damage state failure cost in present value, P_k is the probability of the k^{th} loading state being reached at the time of loading, λ is the annual discount rate, N is the annual event occurrence rate (simple Poisson process modeling), k is the total number of damage states under consideration, and C_m are operation and maintenance costs per year.

For the preliminary analysis executed in this paper, a number of values within Equation 4 are simplified for the sample bridge system shown in Figure 9. The only “costs” being considered are primary energy (PE) consumption in MJ and global warming potential emissions (GWP) measured in kg $\text{CO}_2\text{-eq}$. The initial costs of each retrofit system in terms of PE and GWP were given in Table 2. For simplicity, a small set of earthquake events (with modeled return periods) are applied to the system. Since the post-event damage states are defined equally for each event, the damage failure state costs, C_k , are also assumed equal and therefore left out of the comparative impact calculations. In this analysis, the primary energy and global warming potential impacts are not discounted since all impacts occur in the present assumption. Regardless, Weitzman [37] has also suggested that such long-lasting impacts for environmental indicators be discounted at the lowest possible amounts. However, the variability and inclusion of discount rates for environmental impacts is a topic of future research. Finally, maintenance and operation costs, C_m , are assumed to be zero for the service life of the system since all of the retrofits are intended to be

installed and received little or no maintenance after construction.

4 RESULTS

The annualized total bridge impact (per year or expected service life) for each retrofit system is shown in Table 3. Only the results for no damage, moderate damage, and complete collapse are shown for brevity. These results are broken down into (a) moderate, (b) severe, and (c) weak seismic events.

Table 3: Annualized global warming potential (GWP) and primary energy (PE) impacts per bridge for each retrofit as a function of magnitude and damage state

		GWP (kg CO ₂ -e/yr)	PE (MJ/yr)
Weak Event	UPR-based Wrapping	0.132	0.606
	Epoxy-based Wrapping	0.048	5.55
	Steel Jacket	1.98	31.7
Moderate Event	UPR-based Wrapping	0.144	0.102
	Epoxy-based Wrapping	0.048	0.072
	Steel Jacket	2.28	21.7
Strong Event	UPR-based Wrapping	0.030	0.696
	Epoxy-based Wrapping	0.012	1.428
	Steel Jacket	0.552	8.70

(a) Annualized impacts for a damage state of “no discernible damage”

		GWP (kg CO ₂ -e/yr)	PE (MJ/yr)
Weak Event	UPR-based Wrapping	0.30	0.66
	Epoxy-based Wrapping	0.012	1.18
	Steel Jacket	0.36	5.28
Moderate Event	UPR-based Wrapping	0.07	1.49
	Epoxy-based Wrapping	0.024	2.81
	Steel Jacket	0.96	15.1
Strong Event	UPR-based Wrapping	0.018	0.41
	Epoxy-based Wrapping	0.006	0.81
	Steel Jacket	0.288	4.58

(b) Annualized impacts for “moderate damage” state

		GWP (kg CO ₂ -e/yr)	PE (MJ/yr)
Weak Event	UPR-based Wrapping	0.004	0.08
	Epoxy-based Wrapping	0.0006	0.13
	Steel Jacket	0.024	0.35
Moderate Event	UPR-based Wrapping	0.024	0.52
	Epoxy-based Wrapping	0.006	0.77
	Steel Jacket	0.084	1.39
Strong Event	UPR-based Wrapping	0.006	0.13
	Epoxy-based Wrapping	0.002	0.18
	Steel Jacket	0.023	0.372

(c) Annualized impacts for “complete collapse” state

From these results some trends emerge. These include:

- (1) In all cases, the annualized impacts of FRP seismic retrofitting are lower than for steel jacketing.
- (2) For the lower damage state protection, unsaturated polyester resin and epoxy-based resin retrofitting systems become more efficient (i.e. lower annualized impact) as the expected event magnitude grows.
- (3) At higher damage states (complete collapse) the trends of higher efficiency among FRP alternatives (i.e. lower annualized impact) with higher ground motion is not consistent.
- (4) Unsaturated polyester-based FRP wrapping is more efficient than epoxy-based FRP wrapping and in all cases at all ground motion intensities with regard to annualized primary energy consumption.
- (5) Epoxy-based FRP wrapping is more efficient than unsaturated polyester-based FRP wrapping in all cases and at all ground motion intensities with regard to annualized global warming gas emissions.

5 CONCLUSIONS

Within this paper a methodology for the sustainability assessment of seismic retrofitting techniques was presented. In this early stage of work, two sustainability impacts, annualized global warming potential emissions (measured in CO₂-eq) and primary energy consumption (MJ), were measured for three seismic retrofitting techniques for bridge applications. These techniques were column jacketing using steel jackets, epoxy-based fiber reinforced polymer wrapping, and unsaturated

polyester-based fiber reinforced polymer wrapping. Ultimately, a quantitative comparison between each of these retrofitting techniques was carried out for a variety of expected damage states and ground motion intensities.

One major part of this study included the construction of a life cycle inventory for unsaturated polyester resin (UPR) produced in the United States. This effort required primary data collection about the process steps, raw material requirements, and emissions associated with the large-scale production of UPR. While a complete life cycle inventory has been constructed, only two impact indicators are used in this study, global warming potential and primary energy consumption.

A second major part of this study focused on the use of seismic hazard assessment and structural fragility curves to determine the annualized impact of the various seismic retrofitting techniques. At the center of this analysis is the use of fragility curves to assess the probability of damage due to a range of seismic events, and pairing that risk of damage with the impacts accrued during the retrofitting production and application stages.

Final results showed that in all cases, the annualized impacts of fiber-reinforced polymer (UPR or epoxy-based) were lower than that for steel jacketing. However, the results between UPR and epoxy-based retrofitting were mixed depending on the sustainability indicator chosen (global warming potential or primary energy consumption).

A great deal of additional work is planned with regard to this effort. This work will include the consideration of secondary impacts (i.e. impacts of construction shutdowns and associated disruptions) as discussed by Kiremidjian et al [28], the likelihood of unequal damage states among retrofitting techniques for a given seismic event, the introduction of discount rates for environmental impacts, the introduction of operations and maintenance costs associated with maintaining a retrofit application, an overall comparison with economic life cycle cost, inclusion of additional environmental indicators, and an optimization algorithm to enable efficient design of sustainable seismic retrofitting on a structure, region, or network level scale. Other seismic retrofitting techniques, such as girder ties could also be considered.

This paper represents an initial effort to determine the sustainability impacts of various seismic retrofitting techniques for transportation infrastructure similar to the ways in which economic costs have been calculated and optimized by others. As infrastructure owners and managers become more cognizant of the comprehensive sustainability impacts of their systems, such approaches to the design and management of infrastructure in seismic regions are likely to become more widely used and accepted.

ACKNOWLEDGEMENTS

The authors would like to gratefully acknowledge Mr. Tom Stewart, Dr. Enio Kumpinsky, and Mr. Nick Frieden, for their assistance in putting together the US-based unsaturated polyester resin life cycle inventory.

REFERENCES

- [1] M.J.N. Priestley, F. Seible, G.M. Calvi: Seismic design and retrofit of bridges, John Wiley & Sons Inc., pp. xv (1996)
- [2] S.-H. Kim, M. Shinozuka: Development of fragility curves of bridges retrofitted by column jacketing, Probabilistic Engineering Mechanics, Vol. 19, pp. 105-112 (2004)
- [3] M. Shinozuka, S.-H. Kim, S. Kushiyama, J.-H. Yi: Fragility curves of concrete bridges retrofitted by column jacketing, Earthquake engineering and engineering vibration, Vol. 1, No. 2, pp. 195-205 (2002)
- [4] J. E. Padgett, R. DesRoches: Retrofitted bridge fragility analysis for typical classes of multi-span bridges, Earthquake Spectra, Vol. 25, No. 1, pp. 117-141 (2009)
- [5] Caltrans: Seismic retrofit program fact sheet. State of California, Website: <http://www.dot.ca.gov/hq/paffairs/about/retrofit.htm>. Accessed: August 21, 2009
- [6] F. Seible, M.J.N. Priestley, G.A. Hegemier, D. Innamorato: Seismic retrofit of RC columns with continuous carbon fiber jackets, Journal of Composites for Construction (ASCE), Vol. 1, No. 2, pp. 52-62 (1997)
- [7] M.S. Saiidi, F. Matinovic, B. McElhaney, D. Sanders, F. Gordaninejad: Assessment of steel and fiber reinforced plastic jackets for seismic retrofit of reinforced concrete columns with structural flares, Journal of Structural Engineering (ASCE), Vol. 130, No. 4, pp. 609 – 617 (2004)
- [8] Y.H. Chia, M.J.N. Priestley, F. Seible: Seismic retrofit of circular bridge columns for enhanced flexural performance, ACI Structural Journal, Vol. 8, No. 5, pp. 572-584 (1991)
- [9] M.J.N. Priestley, F. Seible, Y. Xiao, R. Verma: Retrofitting of reinforced concrete bridge columns for enhanced shear strength – part 2: test results and comparison with theory, ACI Structural Journal, Vol. 91, No. 5, pp. 537-551 (1994)
- [10] A. Ghobarah, T.S. Aziz, A. Biddah: Rehabilitation of reinforced concrete frame connections using corrugated steel jacketing, ACI Structural Journal, Vol. 94, No. 3, pp. 282-294 (1997)
- [11] H. Saadatmanesh, M.R. Ehsani, L. Jin: Seismic

- strengthening of circular bridge pier models with fibre composites, *ACI Structural Journal*, Vol. 13, No. 2, pp. 639-647 (1996)
- [12] J.G. Teng, J.F. Chen, S.T. Smith, L. Lam: FRP-strengthened RC structures, John Wiley & Sons Inc., (2002)
- [13] C.E. Bakis, L.C. Bank, V.L. Brown, E. Cosenza, J.F. Davalos, J.J. Lesko, A. Machida, S.H. Rizkalla, T.C. Triantafillou: Fiber reinforced polymer composites for construction – state-of-the-art review, *Journal of Composites for Construction*, Vol. 6, No. 2, pp. 73-87 (2002)
- [14] K.-S. Youm, H.-E. Lee, S. Choi: Seismic performance of repaired RC columns, *Magazine of Concrete Research*, Vol. 58, No. 5, pp. 267-276 (2006)
- [15] International Organization for Standardization: Environmental management – life cycle assessment – principles and framework, International Organization for Standardization, Geneva. (1997)
- [16] A.J. Kappos, E.G. Dimitrakopoulos: Feasibility of pre-earthquake strengthening of buildings based on cost-benefit and life cycle cost analysis with the aid of fragility curves, *Natural Hazards*, Vol. 45, pp. 33-54 (2008)
- [17] P. Hofstetter: Perspectives in Life Cycle Impact Assessment – A structure approach to combine models of the technosphere, ecosphere, and valuesphere, Kulwer Academic Press, Boston (1998)
- [18] J.C. Bare, T.P. Gloria: Critical analysis of the mathematical relationships and comprehensiveness of life cycle impact assessment approaches, *Environmental Science and Technology*, Vol. 40, No. 4 (2006)
- [19] European Commission: International Reference Life Cycle Data System (ILCD) Handbook: Specific guidance document for generic or average Life Cycle Inventory (LCI) data sets, pg 1-103. 1 June 2009 (draft)
- [20] Intergovernmental Panel on Climate Change (IPCC): Fourth Assessment Report (AR4) Geneva, Switzerland (2007)
- [21] APME: Eco-profiles of European Plastics Industry, Accessed 13 May 2009. <<http://lca.plasticseurope.org/styr4.htm>>
- [22] R. G. Hunt et al.: Life Cycle Assessment of Ethylene Glycol and Propylene Glycol Antifreeze, Technical Paper Series, The Engineering Society for Advancing Mobility Land Sea Air and Space, International Congress & Exposition, Detroit, MI, 26-29 Feb. 1996
- [23] X. Domènech, J. A. Ayllón, and J. Peral: How Green Is a Chemical Reaction: Application of LCA to Green Chemistry, *Environmental Science & Technology*, Vol. 36, No. 24, pp. 5517-5520 (2002)
- [24] Franklin Associates, Ltd: Energy consumption and emissions for energy production and transport, Prairie Village (1998)
- [25] SimaPro, PRé Consultants, Netherlands. (2008)
- [26] S. Kim and B. E. Dale: Life Cycle Inventory Information of the United States Electricity System, *International Journal of LCA*, Vol. 10, No. 4, pp. 294-304 (2005)
- [27] J.B. Mander, M.J.N. Prestley, R. Park: Theoretical stress-strain model for confined concrete, *Journal of Structural Engineering (ASCE)*, Vol. 114, No. 8, pp. 1804-1826 (1988)
- [28] A.S. Kiremidjian, Y. Fan, A. Hortacu, K. Burnell, J. LeGrue: Earthquake risk assessment for transportation systems – analysis of pre-retrofitted system, 7th International Conference on Earthquake Engineering, Boston (2002)
- [29] M. Shinozuka, Y. Murachi, X. Dong, Y. Zhou, M.J. Orliowski: Seismic performance of highway transportation networks, China-US Workshop on Protection of Urban Infrastructure and Public Buildings against Earthquakes and Manmade Disasters, Beijing (2003)
- [30] S.D. Werner, C.E. Taylor, J.E. Moore, J.S. Walton, S. Cho: A risk-based methodology for assessing seismic performance of highway systems, Technical Report MCEER-00-0014, MCEER (2000)
- [31] P. Grossi: Earthquake damage assessment – from expert opinion to fragility curves, 8th ASCE specialty conference on probabilistic mechanics and structural reliability (2000)
- [32] M. Shinozuka, M.Q. Feng: Nonlinear static procedure for fragility curve development, *Journal of Engineering Mechanics (ASCE)*, Vol. 126, No. 12, pp. 1287-1295 (2000)
- [33] A. Dutta, J.B. Mander: Seismic fragility of highway bridges, Proceedings of the Center-to-Center Project Workshop on Earthquake Engineering in Transportation Systems, Tokyo (1999)
- [34] Y.K. Wen, Y.J. Kang: Minimum building life-cycle cost design criteria I – methodology, *Journal of Structural Engineering (ASCE)*, Vol. 127, No. 3, pp. 330-337 (2001)
- [35] D.M. Frangopol, J.S. Kong, E.S. Garaibeh: Reliability-based life-cycle management of highway bridges, *Journal of Computing in Civil Engineering*, Vol. 15, No. 1, pp. 27-34 (2001)
- [36] M. Liu, S.A. Burns, Y.K. Wen: Optimal seismic design of steel frame buildings based on life cycle cost considerations, *Earthquake Engineering and Structural Dynamics*, Vol. 32, pp. 1313-1332 (2003)
- [37] M.L. Weitzman: Why the far-distant future should be discounted at its lowest possible rate, *Journal of Environmental Economics and Management*, Vol. 39, pp. 201-208 (1998)